



The potential of nanocomposites (patuletin-conjugated with gallic acid-coated zinc oxide) against free-living amoebae pathogens

Ruqaiyyah Siddiqui^{1,2} · Bushra Khatoun³ · Muhammad Kawish³ · Sreedevi Sajeev⁴ · Shaheen Faizi³ · Muhammad Raza Shah³ · Ahmad M. Alharbi⁵ · Naveed Ahmed Khan^{2,6}

Received: 29 May 2024 / Revised: 9 August 2024 / Accepted: 13 August 2024
© The Author(s), under exclusive licence to Springer Nature Switzerland AG 2024

Abstract

Free-living amoebae infections are on the rise while the prognosis remains poor. Current therapies are ineffective, and there is a need for novel effective drugs which can target *Naegleria*, *Balamuthia*, and *Acanthamoeba* species. In this study, we determined the effects of a nano-formulation based on flavonoid patuletin-loaded gallic acid functionalized zinc oxide nanoparticles (PA-GA-ZnO) against *Acanthamoeba*, *Balamuthia*, and *Naegleria* trophozoites. Characterization of the nano-formulation was accomplished utilizing analytical tools, namely Fourier-transform infrared spectroscopy, drug entrapment efficiency, polydispersity index, dimensions, and surface morphologies. Anti-amoebic effects were investigated using amoebicidal assay, cytopathogenicity assay, and cytotoxicity of the nano-formulation on human cells. The findings revealed that nano-formulation (PA-GA-ZnO) displayed significant anti-amoebic properties and augmented effects of patuletin alone against all three brain-eating amoebae. When tested alone, patuletin nano-formulations showed minimal toxicity effects against human cells. In summary, the nano-formulations evaluated herein depicts efficacy versus *Acanthamoeba*, *Balamuthia*, and *Naegleria*. Nonetheless, future studies are needed to comprehend the molecular mechanisms of patuletin nano-formulations versus free-living amoebae pathogens, in addition to animal studies to determine their potential value for clinical applications.

Keywords Nanocomposite · Patuletin-zinc oxide · *Acanthamoeba* · *Balamuthia* · *Acanthamoeba* · Anti-amoebic · Central nervous system infections · Nanotechnology

Introduction

Pathogenic free-living amoebae (FLA) are widely present in the environment and can cause severe infections involving the brain that may affect both immunocompromised individuals as well as healthy individuals (Rice et al. 2020; Sarink et al. 2022; Chaúque et al. 2023; Fuerst 2023). While individuals with weakened immune systems are typically more susceptible to the infection caused by these protists, amoebae like *Balamuthia mandrillaris*, and *Naegleria fowleri* can cause infection in immunocompetent individuals. On the other hand, *Acanthamoeba* species mostly affect people with compromised immunity (Mungroo et al. 2022). In addition to brain infection, *Acanthamoeba* can cause a blinding infection, i.e. *Acanthamoeba* keratitis (AK), particularly among individuals who wear contact lenses (Siddiqui and Khan 2023). Despite being considered as “rare”, pathogenic free-living amoebae have been detected in water supplies globally, and their prevalence in the water supplies is further exacerbated with the additional challenge of global warming,

✉ Naveed Ahmed Khan
naveed5438@gmail.com

- ¹ Institute of Biological Chemistry, Biophysics and Bioengineering, Heriot-Watt University, Edinburgh EH14 4AS, UK
- ² Microbiota Research Center, Istinye University, Istanbul 34010, Turkey
- ³ International Center for Chemical and Biological Sciences, H.E.J. Research Institute of Chemistry, University of Karachi, Karachi 75270, Pakistan
- ⁴ Research Institute of Medical and Health Sciences, University of Sharjah, 27272 Sharjah, United Arab Emirates
- ⁵ Department of Clinical Laboratories Sciences, College of Applied Medical Sciences, Taif University, P.O. Box 11099, 21944 Taif, Saudi Arabia
- ⁶ School of Science, College of Science and Engineering, University of Derby, Derby, UK DE22 1GB

as amoebae are thermophilic (Baumgartner et al. 2003). Furthermore, due to their phagotrophic nutrition, amoebae have the ability to consume and interact with various potential pathogens including viruses, bacteria, fungi, and/or protozoa (Balczun et al. 2017; Rayamajhee et al. 2021).

At present, a cocktail of various drugs is typically utilized consisting of azoles (fluconazole, ketoconazole, and itraconazole) and amphotericin B, pentamidine or sulfamides, or miltefosine. Additionally, antibacterials such as rifampicin, macrolides, and their derivatives are employed (Mungroo et al. 2019; Cope et al. 2020). Nonetheless, the available medications are usually ineffective as evidenced from the high mortality rate of more than 90%, if the central nervous system (CNS) is involved and/or severe side effects (Ong et al. 2017; Balczun et al. 2017; Debnath 2021; Rice et al. 2020). For example, nephrotoxicity or hepatotoxicity may be observed, as these drugs are required in high doses to be able to cross the blood–brain barrier, in order to reach the site of infection to target the pathogen (Ong et al. 2017; Gabriel et al. 2019).

Nature is an unlimited source of molecules which are used in drug development due to their bioactivity. For centuries, natural products are the backbone of traditional medicine and have been employed to control or treat a variety of human ailments (Clardy and Walsh 2004). Mainly, it furnished a vast library of phytochemicals that can be explored as anti-parasitics. In this regard, several flavonoids have been investigated as viable options for anti-FLA in drug development (Siddiqui et al. 2021). Flavonoids have been extracted from plants and plant-derived products. They have gained interest as promising treatment options for protozoan parasites such *Entamoeba histolytica*, *Trypanosoma cruzi*, *Cryptosporidium parvum*, and *Giardia intestinalis* (Lê et al. 2023). Previously, flavonoids were tested for in vitro anti-amoebic potential against *N. fowleri* and *Acanthamoeba* species. Among all the flavonoids, kaempferol, Afzelin, and quercetin, were tested against *N. fowleri* and *Acanthamoeba*. Kaempferol showed significant anti-amoebic effects versus *N. fowleri* and *Acanthamoeba* species but abelein showed limited effects (Lê et al. 2023). When conjugated with silver, quercetin-conjugated silver nanoparticles showed anti-amoebic properties against *Acanthamoeba* (Anwar et al. 2020).

Patuletin is one of the major flavonoids found in the *T. patula*. It was first isolated by Rao and Seshadri in 1941 from the petals of *T. patula* and represented as 3,5,7,3',4'-pentahydroxy-6-methoxy flavone. PA has many biological features such as antioxidant, antibacterial analgesic, anti-inflammatory, cytotoxic, genotoxic, hepatoprotective, antiproliferative, antinociceptive, antiplatelet, and antihypertensive effects (Corrêa et al. 2018; Faizi et al. 2008; Patel et al. 2024; Sadaf et al. 2023). In addition, PA has been used in the development of nanocarriers. The recent reports highlight that PA can produce stable and biocompatible nanoparticles. These

nanoparticles may effectively transport medications to specific areas in the body when combined with other substances (Ateeq et al. 2015; Jabeen et al. 2016; Razzak et al. 2023a, 2023b).

Nanotechnology may offer a potential solution to various challenges in treating infections (Kirtane et al. 2021) and has shown promise against FLA infections (Padzik et al. 2018; Siddiqui et al. 2023; Latifi et al. 2024). Formulating novel or existing drugs may address issues like reduced bioavailability, weak drug accumulation in the infected site, and poor prognosis due to side effects (Masri et al. 2019; Kirtane et al. 2021). Metal nanoparticles, such as zinc oxide (ZnO), are inexpensive and easily functionalized and exhibit intrinsic antibacterial potential (Souza et al. 2020; Jones et al., 2008; Lee et al. 2019). Gallic acid (GA), also known as 2,4,5-trihydroxy benzoic acid, is a very prevalent compound of plant origin. Classified as phenolics, it exhibits several pharmacological properties including antioxidant, antibacterial, anticancer, and numerous others (Kakheshani et al., 2019; Selvaraj et al., 2022). Because of its appealing pharmacological characteristics and reactive structural framework, it can be efficiently combined with different molecules like peptides and antibiotics (Nourah et al., 2020; Al-Zahrani et al., 2020). Additionally, it can be functionalized on various nanocarriers, resulting in a synergistic effect against a wide range of conditions (Hassani et al. 2020; Azhar et al., 2020; Ghodake et al., 2020).

The overall aim of this study was to determine the effect of a nano-formulation based on flavonoid, PA-loaded GA-functionalized ZnO nanoparticles (PA-GA-ZnO) against the trophozoite stage of *Acanthamoeba*, *Balamuthia*, and *Naegleria*.

Materials and methods

The acquired solvents for this study are of HPLC grade and purchased from Sigma-Aldrich (USA) through a local supplier. Zinc chloride (ZnCl₂), sodium hydroxide (NaOH), and GA were also purchased from Sigma-Aldrich (USA).

Isolation of patuletin

Patuletin was extracted from *Tagetes patula* flowers using a procedure that was previously reported (Faizi et al., 2011). In summary, a total of 4.5 kg of fresh *T. patula* flowers was subjected to sequential extraction using petroleum ether (PE), dichloromethane (DC), ethyl acetate (EA), and acetone. This process was carried out twice at room temperature. The EA extract was evaporated under a vacuum, resulting in a concentrated

material. This extract was then separated into numerous purified fractions using vacuum liquid chromatography. One of these fractions produced a yellow solid substance after being stored for a few days at ambient temperature. The substance was then filtered and washed many times with PE, followed by DC and EA, resulting in the isolation of pure PA (7 g) (Ateeq et al. 2015).

Spectra characterization

Patuletin (PA)

State: yellow powder. TLC solvent system: silica gel 60F₂₅₄ (CHCl₃: MeOH 9:1, R_f=0.28) and reverse phase (RP-18: MeOH: H₂O 6:4, R_f=0.34). EIMS *m/z* (%): 332 (M⁺, 100), 314 (26), 289 (74), 137 (46).

EIMS (MAT 312, Finnigan Germany) (*m/z*): 332 [M⁺], 314, 289, 137

¹H NMR, H (400 MHz, C₃D₆O): 3.87 (3H, s, 6-OCH₃), 6.59 (1H, s, 8-H), 7.82 (1H, d, J=2.1 Hz, 2'-H), 6.98 (1H, d, J=8.5 Hz, 5'-H), 7.69 (1H, dd, J=2.1, 8.5 Hz, 6'-H), 12.3 (1H, s, 5-OH) disappeared on D₂O shake

¹³C NMR (100 MHz, C₃D₆O): 60.79 (6-OCH₃), 147.14 (C-2), 136.40 (C-3), 176.80 (C-4), 153.12 (C-5), 131.72 (C-6), 157.79 (C-7), 94.53 (C-8), 152.39 (C-9), 104.58 (C-10), 123.86 (C-1'), 115.82 (C-2'), 145.75 (C-3'), 148.30 (C-4'), 116.22 (C-5') 121.55 (C-6').

Development of surface-coated GA-ZnO and PA-loaded (PA-GA-ZnO)

Surface-modified GA-ZnO nanoparticles were synthesized using a modified version of a previously published procedure (Cháuque et al. 2023). In brief, 1.5 g of GA and 6 g of ZnCl₂ (15 mM) were introduced into a 250-mL conical flask containing a solution of methanol and water. The mixture was continuously mixed for 30 min. Afterward, a 10% solution of NaOH was gradually added until the pH value of 12–13. The mixture was then rapidly agitated for 4 h, resulting in a white precipitate of GA-ZnO. The solution was centrifuged at a speed of 12,000 × g for 15 min. It was then rinsed three times with deionized water and subjected to calcination at a temperature of 400 °C for a period of 2 h. The resultant white solid was stored for further investigation. The incorporation of PA into GA-ZnO was conducted. In brief, a solution of PA (1 mg/mL) was prepared using methanol and then mixed with a fixed concentration of GA-ZnO (2 mg/mL) over a period of 24 h. The PAT-GA-ZnO was subjected to centrifugation at a speed of 12,000 × g. The resulting liquid portion, which included unbound PA, was then examined using a UV–VIS spectrometer (Thermo Scientific Evolution 220, Shanghai, China) at a wavelength of 292 nm.

Hydrodynamic diameter, polydispersity index (PDI), and morphology

The size and PDI of GA-ZnO and PA-GA-ZnO were examined using a Zetasizer instrument (ZetasizerNano ZS90, Malvern Instruments, Malvern, UK). In general, nanosuspensions (0.1 mg/mL) were transferred to plastic cuvettes, and mediums' viscosity, pressure, and refractive index were adjusted to 1.0, 80.4, and 1.33, respectively. GA-ZnO and PAT-GA-ZnO were examined for surface morphology study using Atomic Force Microscopy (AFM, Agilent 5500, Agilent, USA).

Drug loading efficiency

The drug loading efficiency was carried out as previously described (Akbar et al., 2022). Briefly, the PA-GA-ZnO nano-suspensions were centrifuged at 12,000 × g for 15 min in order to separate nanoparticles. The supernatant was diluted many times and then examined using a UV–VIS spectrophotometer at 292 nm. The percentage of drug entrapment capability of PA was determined employing the following relation:

$$\% \text{ Drug loading} = \frac{(\text{Amount of drug used} - \text{Unloaded drug})}{(\text{Amount of drug used})} \times 100$$

$$\frac{\text{Amount of drug used} - \text{Unloaded drug}}{\text{Amount of drug used}} \times 10$$

Fourier-transform infrared spectroscopy (FT-IR) analysis

The FT-IR spectra of powdered samples of PA, GA-ZnO, and PA-GA-ZnO were obtained using a Shimadzu IR-470 spectrometer (Shimadzu, Kyoto, Japan) with a resolution of 4 cm⁻¹. The sample preparation was conducted using the KBr disc technique. The air-dried materials were combined with potassium bromide and then compressed at a pressure of 200 psi to create a self-supporting palette. The spectra were analyzed within the frequency range of 400–4000 cm⁻¹.

In vitro release study

In vitro release of PA in buffer solution (pH 7.0 and 5.0) containing 1% Tween 80 was conducted using the dialysis method. Briefly, 2 mL of drug-loaded nanoparticles (2.5 mg/mL) PA-GA-ZnO exposed on the buffer (pH 7.0 and 5.0) and transferred in dialysis bag after fixing at both ends. The membrane was placed in a beaker containing 40 mL buffer media (pH 7.0 and 5.0) and allowed to shake at 100 × g/

min at 37 °C. Aliquots (2 mL) were withdrawn at specific time intervals and replaced with fresh buffer to prevent drug saturation. The PA release content was quantified at different time intervals via UV–Vis spectrophotometer at λ max 292 nm.

Human cerebral microvascular endothelial cells (HBEC-5i)

The cells were purchased from the American Type Culture Collection (ATCC cat. no. CRL-3245). As per ATCC, HBEC-5i were originally derived from the cerebral cortex of a patient and immortalized by transfection with a plasmid containing SV40 large T antigen, and exhibits endothelial cell markers such as VE-cadherin, von Willebrand factor VIII, occludin, CD54, CD40, and tight-junctions as determined by low permeability to 70 kDa dextran. HBEC-5i provide an excellent continuous resource of cerebral microvascular endothelial cells as a replacement for primary brain endothelial cells. Cells are routinely cultured in dedicated media, such as Dulbecco Modified Eagle Medium/Nutrient Mixture F-12 (DMEM/F-12), supplemented with glucose, L-glutamine, sodium pyruvate, foetal bovine serum, and endothelial cell growth supplement in T-75 cm³ tissue culture flasks at 37 °C in a 5% CO₂ incubator with over 95% humidity (Alvi et al. 2023). Once a complete cell monolayer was formed, cells were dislodged using trypsin and the cell pellet was obtained by centrifugation at 2500 g for 5 min and used for assays. For various assays, 50,000 cells/well were grown in 96-well plates.

Acanthamoeba castellanii cultivation

Acanthamoeba castellanii of the genotype T4 (ATCC cat. no. 50492) are routinely cultured in 10 mL PYG media (0.75% proteose peptone, 0.75% yeast extract, and 1.5% glucose) at 30 °C in T-75 cm³ tissue culture flasks. Under these conditions, amoebae trophozoites adhere to the flask. Once confluent, flasks were placed on ice for 20 min to detach amoebae. Next, amoebae were collected by gentle tapping for 5 min before being examined under an inverted light microscope. After collecting the suspension in a 15-mL tube, amoebae were centrifuged for 10 min at 2500 × g. Finally, amoebae pellet was resuspended in 1 mL of RPMI, and amoebae were enumerated with a haemocytometer and used in subsequent assays (Anwar et al. 2020).

Cultures of *Naegleria fowleri*

Naegleria fowleri strain HB1 was obtained from ATCC (cat. no. 30174) and cultured as previously reported (Mungroo

et al. 2020; Siddiqui et al. 2020). Briefly, parasites (1×10^5 amoebae) were inoculated on human cell monolayers grown in tissue culture flasks as a feed. Flasks were incubated at 37 °C in a 95% humidified incubator with 5% CO₂. After 48 h, parasites consumed human cells, resulting in approximately 5×10^5 amoebae, 95% of which were trophozoites (Mungroo et al. 2020; Siddiqui et al. 2020).

Balamuthia mandrillaris cultures

A clinical isolate of *Balamuthia mandrillaris* (ATCC 50209) was originally derived from Papio sphinx, a 3-year-old female mandrill, who died of amoebic meningoencephalitis at the San Diego Zoo (Visvesvara et al. 1993; Mungroo et al. 2020). As before, *B. mandrillaris* (10^5 parasites) were inoculated on human cells as a feeder layer in a CO₂ incubator at 37 °C for 48 h. *B. mandrillaris* consumed human cells, resulting in approximately 5×10^5 parasites (Mungroo et al. 2020).

Amoebicidal assays

Amoebicidal assays were performed as described previously (Mungroo et al. 2020) to determine the effects of drugs and their nanoconjugants. Briefly, approximately 2×10^5 *A. castellanii*, 2×10^5 *B. mandrillaris*, and 2×10^5 *N. fowleri* were incubated with 100 µg per mL of the compound and its nanoconjugants. Negative controls consisted of amoebae alone, whereas positive controls were 50 µM Chlorhexidine as a positive control, and an appropriate volume of water and dimethyl sulfoxide (DMSO) was included as controls. Trypan blue exclusion test was performed to determine the viable amoebae as described below (Aqeel et al. 2013).

Cytotoxicity assays

Cytotoxicity assays were carried out as described previously (Jeyamogan et al. 2018). Briefly, HBEC-5i were grown in 96-well plates in a 5% CO₂ incubator, with 95% humidity at 37 °C for 24 h. Subsequently, cells were incubated with drugs and their nanoconjugants. Finally, the supernatant was harvested and the amount of released lactate dehydrogenase (LDH) was determined using the cytotoxicity detection kit. The inclusion of both negative and positive controls ensured the accuracy of the results and results were calculated as follows: % cell cytotoxicity = (sample value – negative control value) / (positive control value, i.e. 1% Triton X-100 treated – negative control value) × 100.

Host cell cytopathogenicity assay

As previously described, the cytopathogenicity of host cells in response to amoebae was determined using the Lactate

dehydrogenase (LDH) assay (Akbar et al. 2024). Briefly, 2×10^5 *A. castellanii*, 2×10^5 *B. mandrillaris*, and 2×10^5 *N. fowleri* were treated with drugs and their nanoconjugates in RPMI-1640 for 2 h at 30 °C. Next, amoebae were centrifuged for 10 min at $1000 \times g$ and resuspended in 200 μ L RPMI-1640. Pre-treated parasites were inoculated onto human cell monolayers grown in 96-well plates for up to 24 h. The supernatants were collected and the amount of released LDH was estimated to determine the level of host cell damage and the percentage cytopathogenicity was determined as described for cytotoxicity assays.

Results

Synthesis of GA-ZnO and PA-GA-ZnO

The current study was conceptualized to develop surface-functionalized ZnO nanoparticles that possess inherited antiparasitic potential. For this purpose, GA was used as a coating agent, which belongs to a class phenolic compound that possesses a phenolic part along with a carboxylic part. Several studies reported antibacterial, anticancer, and anti-amoebic activity (Keyvani-Ghamsari et al. 2023; Mahboob et al. 2020). The resultant GA-coated ZnO was further loaded with a flavonoid PA to develop the desired PA-GA-ZnO formulation as depicted in (Fig. 1). The developed nanoparticles were characterized by FTIR spectroscopy. The FTIR spectra of GA-ZnO show corresponding peaks of carboxylic moiety (OH) at $3600\text{--}2800\text{ cm}^{-1}$ and a phenolic hydroxyl moiety at 3310 cm^{-1} . The C=O and C=C stretching was also observed at 1670 cm^{-1} and 1580 cm^{-1} (Fig. 2A) (Lee et al., 2017) along with the peak of Zn–O stretching at 845 cm^{-1} which confirms the functionalization of GA onto the surface of ZnO. The FTIR spectra of PA show corresponding peaks of OH and C=C stretching around 3252 cm^{-1} and 1625 cm^{-1} . Moreover, C–O and C–O–C stretch was also observed at 1295 cm^{-1} and 1151 cm^{-1} which follows the previously reported pattern (Metwaly et al. 2023). When PA was loaded onto PA-GA-ZnO (i.e. PA-GA-ZnO), a slight variation in characteristic absorption values was observed (Fig. 2A), the peak of OH was shifted from 3252 to 3255 cm^{-1} and the peak of C=C was shifted from 1625 to 1617 cm^{-1} . This shows that the loading of PA within GA-ZnO (i.e. PA-GA-ZnO) did not alter the chemical nature of the PA.

Hydrodynamic diameter, PDI, and morphology

To achieve higher drug transportation at the diseased site, a relatively smaller hydrodynamic diameter is considered essential for in vitro and in vivo applications (Saifullah et al. 2021). The therapeutic efficacy and physical stability

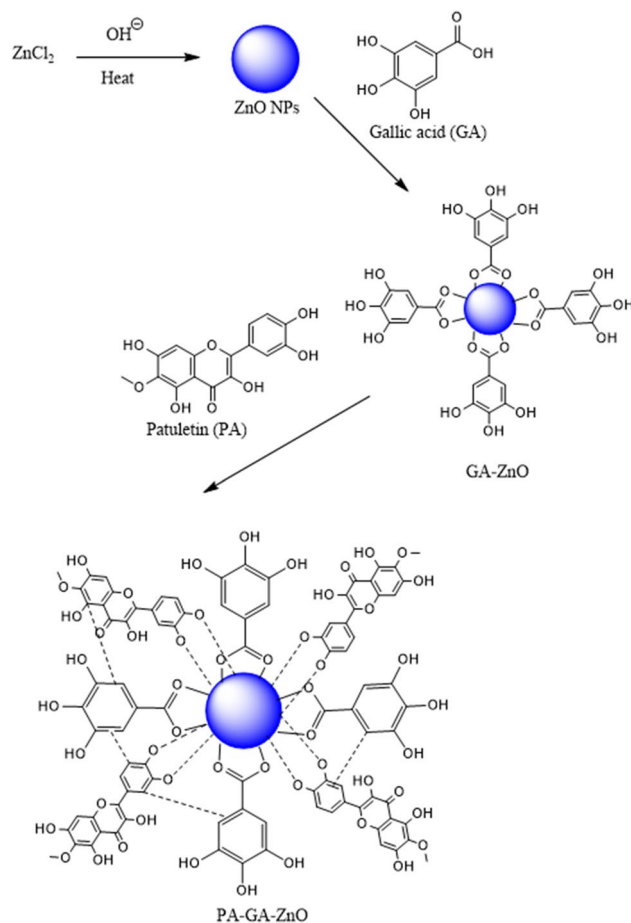


Fig. 1 Synthetic scheme for the preparation of GA-ZnO of PA-GA-ZnO

of the loaded drug are directly influenced by the average diameter, making it an essential and fundamental component of any drug delivery system. The average hydrodynamic diameter and PDI of synthesized GA-ZnO were found to be $170.3 \pm 3.7\text{ nm}$ and 0.205 ± 0.05 (Table 1), respectively. After PA encapsulation, the diameter of the developed PA-GA-ZnO was decreased to $165 \pm 4.2\text{ nm}$ and PDI to 0.180 ± 0.04 . The decrease in size and PDI may be due to the reduction in aggregation of PA-GA-ZnO formulation due to the increment in intramolecular secondary interaction. The developed GA-ZnO and PA-GA-ZnO showed the PDI values less than 0.25, indicating the uniform colloidal particle size distribution. As per AFM images (Fig. 2B), the developed GA-ZnO and PA-GA-ZnO had nearly spherical morphology which is an indicative for their higher stability.

Entrapment efficiency determination

The key characteristics of a drug delivery system are its drug entrapment efficiency, which is enhanced by increased drug entrapment efficiency and a narrow size

Fig. 2 **A** FTIR spectra of GA-ZnO, PA, and PA-GA-ZnO. **B** Atomic force microscopic images of GA-ZnO and PA-GA-ZnO

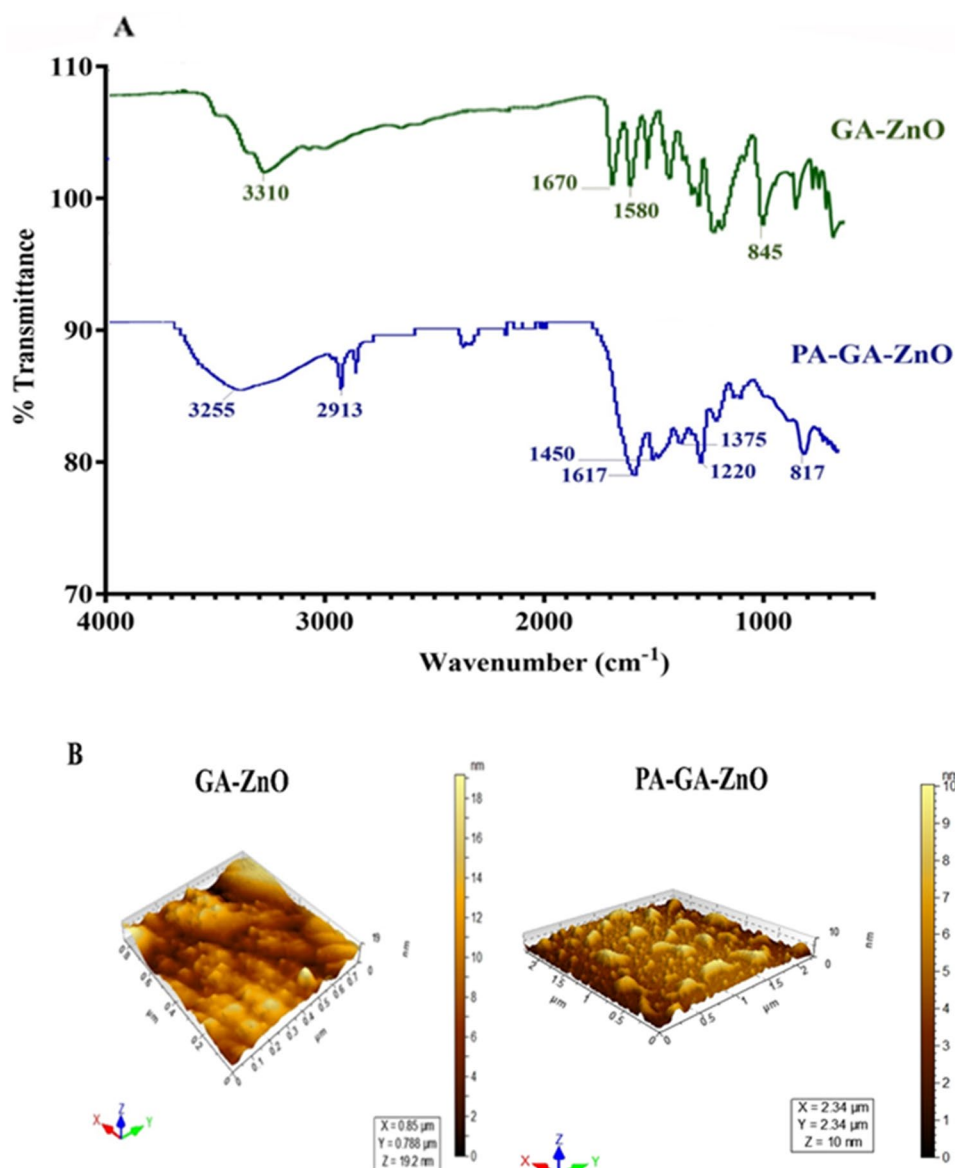


Table 1LE: Table entries for Table 1 were slightly modified. Please check if correct. Otherwise, kindly amend. Also, please check if table citations are presented correctly. Hydrodynamic diameter, polydispersity index, and percent entrapment efficiency of GA-ZnO and PA-GA-ZnO

Nanoparticles	Hydrodynamic diameter (nm)	Polydispersity index (PDI)	% EE
GA-ZnO	170.3 ± 3.7	0.205 ± 0.05	
PA-GA-ZnO	165 ± 4.2	0.180 ± 0.04	55 ± 1.32%

distribution. These attributes facilitate the effective transport of the drug across various biological membranes to the intended site of action (Kawish et al. 2021). The entrapment efficiency of PA-GA-ZnO is shown in (Table 1). PA is a polyphenolic molecule that contains

phenolic hydroxyls and an aromatic backbone. The FTIR spectra indicate a minor shift in the absorption frequencies of OH and C=C, indicating that the entrapment of PA onto GA-ZnO is due to chelation via the OH group and secondary interaction through pi-pi stacking.

In vitro release study

The drug release kinetics is one of the most characteristic features of any drug delivery system. It enables us to analyze the behaviour of developed formulation in different pH conditions. The developed PA-GA-ZnO formulation gives higher release at 51 ± 1.32% (pH 7.0) at 12 h in comparison with the pH 5.0 which was found to be 30.0 ± 0.65% as depicted in (Fig. 3) respectively. PA belongs to a class of flavonoids that possess phenolic moiety in combination with

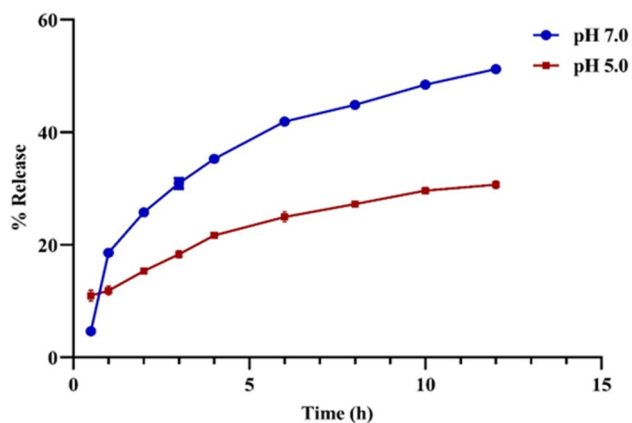


Fig. 3 In vitro release profile of PA from PA-GA-ZnO at pH 7.0 and 5.0

methoxy and carbonyl skeleton. Previous study accounts that the phenolic moiety was a proactive moiety when it comes to chelation with diverse metals. In the present study, secondary interactions and chelation were key factors in encapsulating PA within GA-ZnO. GA on the surface of ZnO forms pi-pi stacking (noncovalent pi interactions, i.e. orbital overlap between the pi bonds of aromatic rings) with PA, and its phenolic and carboxylic groups form hydrogen bonds with PA. These secondary interactions and chelation are also shown by shifts in IR values.

PA-GA-ZnO nanocomposite inhibited parasite viability when tested against pathogenic *A. castellanii*, *B. mandrillaris*, and *N. fowleri*

Amoebicidal effects of ZnO, GA, PA, GA-ZnO, and the conjugated PA-GA-ZnO were tested against pathogenic free-living amoebae. The findings showed that the PA, GA-ZnO, and PA-GA-ZnO-NPs exerted significant amoebicidal effects against *A. castellanii* (Fig. 4A) ($P < 0.05$). In controls, treatment with CHX abolished the viability of *A. castellanii* and no viable amoebae were recorded, while solvent (DMSO)-treatment showed no effects. However, treatment with PA reduced viability by 53%, GA reduced viability by 46%, ZnO reduced viability by 48%, GA-ZnO reduced viability by 61%, and finally, PA-GA-ZnO reduced viability by 69%.

When tested against *B. mandrillaris*, the findings revealed that treatment with CHX abolished the viability of *B. mandrillaris* with 100% amoebicidal effects, while solvent (DMSO)-treatment showed no effects. However, treatment with PA reduced viability by 14%, GA reduced viability by 5%, ZnO reduced viability by 24%, GA-ZnO reduced viability by 60%, and finally, PA-GA-ZnO reduced viability by 90%. Notably, *B. mandrillaris* viability was significantly reduced when GA and PA were conjugated with ZnO i.e. GA-ZnO and PA-GA-ZnO (Fig. 4B) ($P < 0.05$).

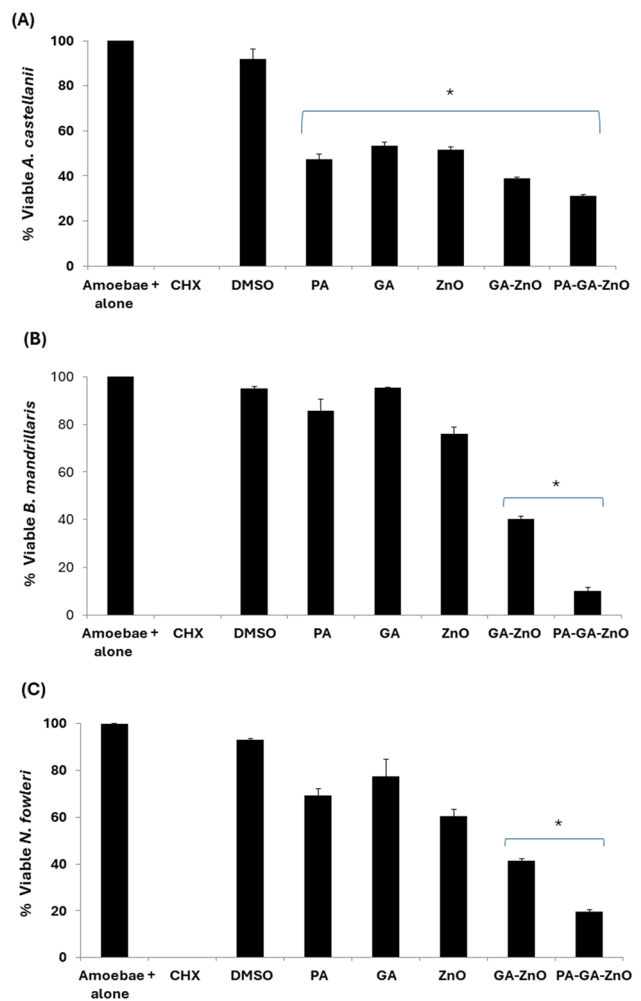


Fig. 4 Patuletin and its nanoconjugates significantly reduced amoebae viability. The amoebicidal effects of various drugs were determined using trypan blue staining. Briefly, amoebae were treated with Patuletin and its nanoconjugates at a concentration of 100 $\mu\text{g}/\text{ml}$ for 24 h at 30 $^{\circ}\text{C}$. The data are presented with a mean \pm standard error and are representative of independent experiments that were conducted. Additionally, p -values were calculated using a two-sample t -test with a two-tailed distribution; the asterisk (*) is $p \leq 0.05$

Against *N. fowleri*, the results revealed that treatment with CHX abolished the viability of *N. fowleri* and no viable amoebae were recorded, while solvent (DMSO)-treatment showed no effects. However, treatment with PA reduced viability by 31%, GA reduced viability by 22%, ZnO reduced viability by 39%, GA-ZnO reduced viability by 59%, and finally, PA-GA-ZnO reduced viability by 80%. Notably, *N. fowleri* viability was significantly reduced when GA and PA were conjugated with ZnO i.e. GA-ZnO and PA-GA-ZnO (Fig. 4C) ($P < 0.05$).

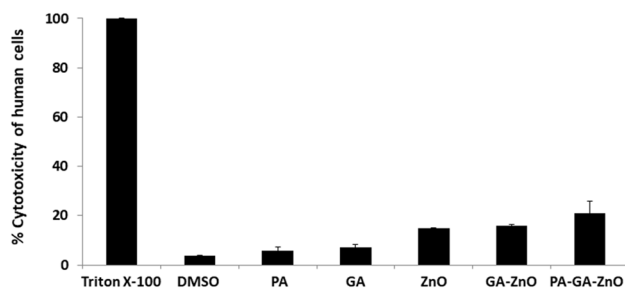


Fig. 5 Cytotoxicity assays were performed to determine the toxicity of patuletin and its nanoconjugates towards HBEC-5i cells as described in the “Materials and methods” section. All the employed compounds displayed limited cytotoxicity. The results are presented as the mean \pm standard error.

Overall, the results revealed that the GA-ZnO and PA-GA-ZnO abolished the viability of all free-living pathogenic amoebae tested in the study.

Nanoconjugates exhibited limited cytotoxicity against human cerebral microvascular endothelial cells

To determine toxic effects of nanoconjugates human cells, cytotoxicity assays were performed. The findings revealed that the nanoconjugates tested exhibited limited cell death against endothelial cells (Fig. 5). The LDH values from cells treated with Triton X-100 were considered 100% cytotoxicity, while negative controls were considered 0% and the sample values were calculated accordingly. Cells treated with DMSO showed 3.8% cytotoxicity, PA treated showed 5%, GA exhibited 7%, ZnO resulted in 15%, GA-ZnO showed 15.8%, and finally PA-GA-ZnO showed 21% cytotoxicity of human cells. Overall the results revealed that the conjugated GA-ZnO and PA-GA-ZnO demonstrated limited cytotoxicity against human brain endothelial cells tested in the study.

Nanoconjugates and their counterparts inhibited parasite-mediated damage to human cerebral microvascular endothelial cells

To determine whether PA, GA, and their nanoconjugates inhibit parasite-mediated human cell damage, cytopathogenicity assays were performed as described in the “Materials and methods” section. The LDH values from cells treated with *A. castellanii* alone were considered 100% cell death, while negative controls were considered 0% and the sample values were calculated accordingly. Pre-treatment of *A. castellanii* with DMSO showed no inhibition and up to 97% host cell death was observed. While amoebae treatment with PA reduced host cell death to 45%, pre-treatment with

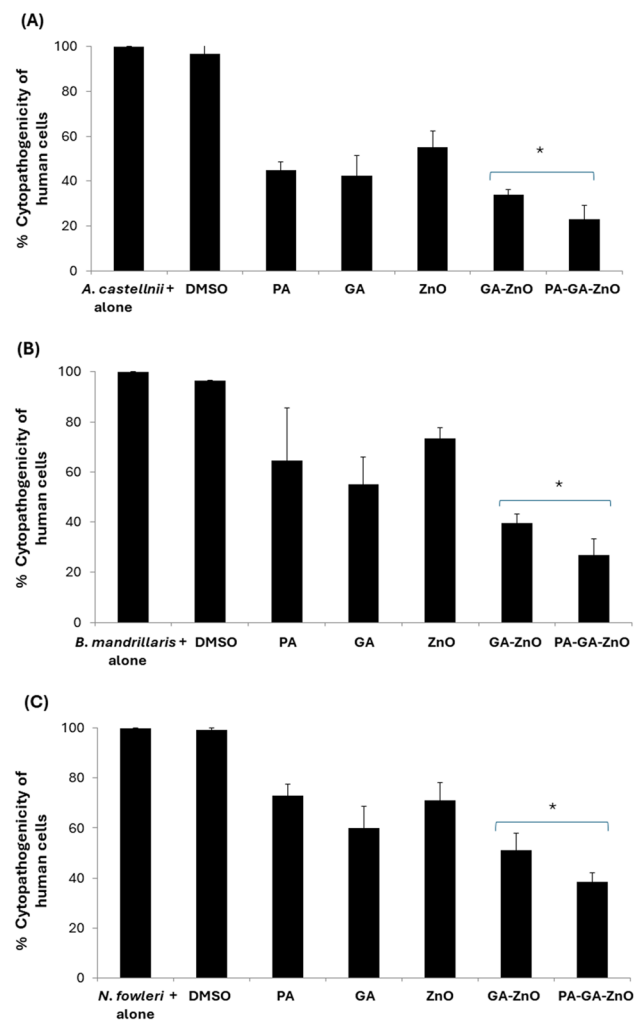


Fig. 6 Patuletin and its nanoconjugants showed a cytopathogenic effect against human cells. After being treated with 100 μ g/ml compounds for 2 h, the compounds showed varying degrees of a reduction in amoebae-mediated host-cell death. The host-cell death was measured after the amoebae were added to the HBEC-5i cell monolayer as described in the “Materials and methods” section; the asterisk (*) is $p \leq 0.05$

GA reduced host cell death to 42%, pre-treatment with ZnO reduced host cell death to 55%, pre-treatment with GA-ZnO reduced host cell death to 34%, and finally pre-treatment with PA-GA-ZnO reduced host cell death to 23% (Fig. 6A).

When *B. mandrillaris* were treated with DMSO, no effects were observed and up to 96% host cell death was observed. While pre-treatment with PA reduced host cell death to 64%, pre-treatment with GA reduced host cell death to 55%, pre-treatment with ZnO reduced host cell death to 73% cell death, GA-ZnO reduced host cell death to 40%, and finally, PA-GA-ZnO reduced host cell death to 27% (Fig. 6B).

For *N. fowleri*, pre-treatment with DMSO showed no inhibition and up to 99% host cell death was observed. However,

parasite treatment with PA reduced cell death to 73%, GA exhibited 60% cell death, ZnO resulted in 71% cell death, GA-ZnO showed 52%, and finally, PA-GA-ZnO showed 38% cell death (Fig. 6C). Overall, the results revealed that the conjugated GA-ZnO and PA-GA-ZnO inhibited host cell death mediated by all pathogenic amoebae tested in this study.

Discussion

Globally, infectious diseases are on the rise (Smith et al. 2014). Infections due to pathogenic free-living amoebae, although deemed as “rare” infections, are of concern, given the escalation of global warming, widescale water shortages, and increasing reliance of the public on water storage tanks, particularly in developing countries, and also the rise in contact lens wearers worldwide, as well as other factors (Angelici et al. 2021; Carnt et al. 2020; Król-Turmińska and Olender 2017; Lorenzo-Morales et al. 2015). Moreover, the true extent of disease burden due to infections caused by free-living amoebae is probably underestimated, given that as much as 60% of encephalitis cases may be going undiagnosed or misdiagnosed as bacterial meningitis cases (Glaser et al. 2003). As current treatments versus these infections are ineffective, there is a need to develop efficacious therapeutic interventions, especially those that can eliminate different types of pathogenic amoebae including *Naegleria*, *Balamuthia*, and *Acanthamoeba*. Flavonoids are generally considered polyhydroxy aromatic compounds rich and possess potential antimicrobial activity against diverse pathogens. Moreover, they are also reported to show potent activities against parasites. For instance, Le et al. 2023 published the antiparasitic activity of diverse flavonoids against *A. castellanii* and *N. fowleri*. They used structurally varied flavonoids such as kaempferol, afzelin, and quercetin, and among them, kaempferol showed good activity against both parasites with an IC_{50} value of about $27.28 \pm 0.22 \mu\text{M}$ and $21.63 \pm 1.28 \mu\text{M}$ against *N. fowleri* and *A. castellanii*, while the rest were inactive.

Patuletin is another flavonoid present in various plants utilized in traditional folk medicine. It exhibits diverse pharmacological effects, such as antioxidative, antibacterial, and anti-inflammatory properties, thus was evaluated for anti-amoebic properties (Razzak et al. 2023).

Our findings indicate that PA-loaded nano-formulation (PA-GA-ZnO) exhibited potent efficacy against pathogenic free-living amoebae, including *N. fowleri*, *B. mandrillaris*, and *A. castellanii*. The flavonoid PA showed 53% inhibition of *A. castellanii*, but when PA was loaded onto GA-ZnO, the inhibition was increased to 61%. Our findings suggest that the integration of the flavonoid patuletin with GA-ZnO resulted in significant anti-amoebic effects. Particularly

noteworthy was the robust antimicrobial impact on *B. mandrillaris*, where amoebae viability was reduced by 90%. The anti-amoebic activities were substantially enhanced in all tested free-living amoebae when the PA was conjugated with GA-ZnO NPs. These outcomes suggest that PA-GA-ZnO can manifest potent anti-amoebic activity, possibly attributed to their surface area and compact size.

Previous studies have indicated that the presence of Gallic acid improves the stability and bioavailability of NPs, suggesting a synergistic effect (Hassani et al. 2020). Additionally, it has been demonstrated that the combination with Gallic acid exhibits stronger antioxidant capabilities compared to each compound individually (Lee et al. 2017; Fiedot-Toboła et al. 2021) which may explain likely mechanisms observed in our findings. Nonetheless, future mechanistic studies should be accomplished to determine the mechanism of action in amoebae.

In summary, the (PA-GA-ZnO) nano-formulation exhibited significant amoebicidal effects against the tested pathogenic free-living amoebae. These results are noteworthy as they demonstrated enhanced biocompatibility with minimal cytotoxicity. The outcomes underscore the potent anti-amoebic activity of the nano-conjugation (PA-GA-ZnO). Our findings suggest that PA-GA-ZnO nano-formulation holds promise for augmenting antimicrobial effects, with potential benefits for bioavailability improvement. Additionally, the nano-formulations demonstrated bactericidal effects against various gram-positive and gram-negative bacteria. This emphasizes the potential of nanoconjugation to address infections caused by pathogenic free-living amoebae and bacteria, serving as a versatile therapy for CNS infections (bacterial and amoebic meningitis cases). However, comprehensive future research utilizing *in vivo* models is essential to ascertain the translational significance of these findings.

Acknowledgements The authors extend their appreciation to Taif University, Saudi Arabia, for supporting this work through project number (TU-DSPP-2024-147).

Author contribution NAK, RS, and SF perceived the study amid discussion with MRS and AMA. SS, BK, and MK conducted all investigations and data analysis under the supervision of NAK, RS, SF, AMA, and MRS. RS and SS wrote the biology part while MK, BK, and SF wrote the chemistry part of the first draft. NAK, AMA and MRS corrected and finalized the manuscript. All authors read and approved the final manuscript.

Funding Ruqaiyyah Siddiqui and Naveed Ahmed Khan are supported by the Air Force Office of Scientific Research (AFOSR). Additionally, this research was funded by Taif University, Taif, Saudi Arabia (TU-DSPP-2024-147).

Data availability The datasets generated during and/or analyzed during the current study are available from the corresponding author on reasonable request.

Declarations

Ethical approval Not applicable.

Conflict of interest The authors declare no competing interests.

References

- Alvi, A., Alqassim, S., Khan, N.A., Khatoun, B., Akbar, N., Kawish, M., Faizi, S., Shah, M.R., Alharbi, A.M., Alfahemi, H. and Siddiqui, R., 2023. Antibacterial effects of quercetagenin are significantly enhanced upon conjugation with chitosan engineered copper oxide nanoparticles. *BioMetals*. 1–14.
- Angelici MC, Walochnik J, Calderaro A, Saxinger L, Dacks JB (2021) Free-living amoebae and other neglected protistan pathogens: health emergency signals? *Eur J Protistol* 77:125760
- Anwar A, Yi YP, Fatima I, Khan KM, Siddiqui R, Khan NA, Anwar A (2020) Antiamoebic activity of synthetic tetrazoles against *Acanthamoeba castellanii* belonging to T4 genotype and effects of conjugation with silver nanoparticles. *Parasitol Res* 119:1943–1954
- Anwar, A., Ting, E. L. S., Anwar, A., Ain, N. u., Faizi, S., Shah, M. R., Khan, N. A., Siddiqui, R. (2020). Antiamoebic activity of plant-based natural products and their conjugated silver nanoparticles against *Acanthamoeba castellanii* (ATCC 50492). *AMB Express*, 10, 1–10.
- Aqeel Y, Siddiqui R, Iftikhar H, Khan NA (2013) The effect of different environmental conditions on the encystation of *Acanthamoeba castellanii* belonging to the T4 genotype. *Exp Parasitol* 135(1):30–35
- Ateeq M, Shah MR, Ain NU, Bano S, Anis I, Lubna Faizi S, Bertino MF, Sohaila Naz S (2015) Green synthesis and molecular recognition ability of patuletin coated gold nanoparticles. *Biosens Bioelectron* 63:499–505. <https://doi.org/10.1016/j.bios.2014.07.076>
- Balczun C, Scheid PL (2017) Free-living amoebae as hosts for and vectors of intracellular microorganisms with public health significance. *Viruses* 9(4):65
- Baumgartner M, Yapi A, Gröbner-Ferreira R, Stetter KO (2003) Cultivation and properties of *Echinamoeba thermanum* n. sp., an extremely thermophilic amoeba thriving in hot springs. *Extremophiles* 7:267–274
- Carnt NA, Subedi D, Connor S, Kilvington S (2020) The relationship between environmental sources and the susceptibility of *Acanthamoeba keratitis* in the United Kingdom. *PLoS ONE* 15(3):e0229681
- Cháuque BJM, da Silva TCB, Dos Santos DL, Benitez GB, Cháuque LGH, Benetti AD, Zanette RA, Rott MB (2023) Global prevalence of free-living amoebae in solid matrices—a systematic review with meta-analysis. *Acta Tropica*. 247:107006
- Clardy J, Walsh C (2004) Lessons from natural molecules. *Nature* 432(7019):829–837
- Cope, J.R., Ali, I.K. and Visvesvara, G.S., 2020. Pathogenic and opportunistic free-living ameba infections. In *Hunter's tropical medicine and emerging infectious diseases* (814–820). Elsevier.
- Corrêa WR, Serain AF, Aranha Netto L, Marinho JVN, Arena AC, de Santana Figueiredo, Aquino D, Kuraoka-Oliveira ÂM, Júnior AJ, Bernal LPT, Kassuya CAL, Salvador MJ (2018) Anti-inflammatory and antioxidant properties of the extract, tiliroside, and patuletin 3-O- β -D-glucopyranoside from *Puffia townsendii* (*Amaranthaceae*). *Evid Based Complement Alternat Med* 2018:6057579. <https://doi.org/10.1155/2018/6057579>
- Debnath A (2021) Drug discovery for primary amebic meningoencephalitis: from screen to identification of leads. *Expert Rev Anti Infect Ther* 19(9):1099–1106
- Faizi S, Siddiqui H, Bano S, Naz A, Lubna Mazhar K, ... Khan SA (2008) Antibacterial and antifungal activities of different parts of *Tagetes patula*: preparation of patuletin derivatives. *Pharm Biol* 46(5):309–320. <https://doi.org/10.1080/13880200801887476>
- Fiedot-Toboła M, Dmochowska A, Potaniec B, Czajkowska J, Jędrzejewski R, Wilk-Kozubek M, Carolak E, Cybińska J (2021) Gallic acid based black tea extract as a stabilizing agent in ZnO particles green synthesis. *Nanomaterials* 11(7):1816
- Fuerst PA (2023) The status of molecular analyses of isolates of *Acanthamoeba* maintained by International Culture Collections. *Microorganisms* 11(2):295
- Gabriel S, Khan NA, Siddiqui R (2019) Occurrence of free-living amoebae (*Acanthamoeba*, *Balamuthia*, *Naegleria*) in water samples in Peninsular Malaysia. *J Water Health* 17(1):160–171
- Glaser CA, Gilliam S, Schnurr D, Forghani B, Honarmand S, Khet-suriani N, Fischer M, Cossen CK, Anderson LJ (2003) In search of encephalitis etiologies: diagnostic challenges in the California Encephalitis Project, 1998–2000. *Clin Infect Dis* 36(6):731–742
- Hassani A, Azarian MMS, Ibrahim WN, Hussain SA (2020) Preparation, characterization and therapeutic properties of gum arabic-stabilized gallic acid nanoparticles. *Sci Rep* 10(1):17808
- Jabeen A, Mesaik MA, Simjee SU, Lubna Bano S, Faizi S (2016) Anti-TNF- α and anti-arthritis effect of patuletin: a rare flavonoid from *Tagetes patula*. In *Immuno Pharmacol* 36:232–240. <https://doi.org/10.1016/j.intimp.2016.04.034>
- Jeyamogan S, Khan NA, Anwar A, Shah MR, Siddiqui R (2018) Cytotoxic effects of Benzodioxane, Naphthalene diimide, Porphyrin and Acetamol derivatives on HeLa cells. *SAGE Open Med* 6:2050312118781962
- Kawish M, Jabri T, Elhissi A, Zahid H, Muhammad Iqbal K, Rao K, Gul J, Abdullah M, Shah MR (2021) Galactosylated iron oxide nanoparticles for enhancing oral bioavailability of ceftriaxone. *Pharm Dev Technol* 26(3):291–301. <https://doi.org/10.1080/10837450.2020.1866602>
- Keyvani-Ghamsari S, Rahimi M, Khorsandi K (2023) An update on the potential mechanism of gallic acid as an antibacterial and anti-cancer agent. *Food Sci Nutr* 11(10):5856–5872. <https://doi.org/10.1002/fsn3.3615>
- Kirtane AR, Verma M, Karandikar P, Furin J, Langer R, Traverso G (2021) Nanotechnology approaches for global infectious diseases. *Nat Nanotechnol* 16(4):369–384
- Król-Turmińska K, Olender A (2017) Human infections caused by free-living amoebae. *Ann Agric Environ Med* 24(2):254
- Latifi A, Esmaeili F, Mohebbi M, Yasami-Khiabani S, Rezaeian M, Soleimani M, Kazemirad E, Amani A (2024) Chitosan nanoparticles improve the effectiveness of miltefosine against *Acanthamoeba*. *PLoS Negl Trop Dis* 18(3):e0011976
- Lê HG, Võ TC, Kang J-M, Nguyễn TH, Hwang B-S, Oh Y-T, Na B-K (2023) Antiamoebic activities of flavonoids against pathogenic free-living amoebae, *Naegleria fowleri* and *Acanthamoeba* species. *Parasites Hosts and Diseases* 61(4):449
- Lee JM, Choi KH, Min J, Kim HJ, Jee JP, Park BJ (2017) Functionalized ZnO nanoparticles with gallic acid for antioxidant and antibacterial activity against methicillin-resistant *S aureus*. *Nanomaterials* 7(11):365
- Lorenzo-Morales, J., Khan, N.A. and Walochnik, J., 2015. An update on *Acanthamoeba keratitis*: diagnosis, pathogenesis and treatment. *Parasite*. 22.
- Mahboob T, Nawaz M, de Lourdes Pereira M, Tian-Chye T, Samudi C, Sekaran SD, Wiat C, Nissapatorn V (2020) PLGA nanoparticles loaded with Gallic acid- a constituent of *Leea indica* against

- Acanthamoeba triangularis. *Sci Rep* 10(1):8954. <https://doi.org/10.1038/s41598-020-65728-0>
- Masri A, Anwar A, Khan NA, Siddiqui R (2019) The use of nanomedicine for targeted therapy against bacterial infections. *Antibiotics* 8(4):260
- Metwaly AM, Abdel-Raouf AM, Alattar AM, El-Zomrawy AA, Ashmawy, AM, Metwally MG, Abu-Saied MA, Lotfy AM, Alsouk BA, Elkaeed EB, Eissa IH (2023) Preparation and characterization of patuletin-loaded chitosan nanoparticles with improved selectivity and safety profiles for anticancer applications. *J Chem* 11:6684015. <https://doi.org/10.1155/2023/6684015>
- Mungroo MR, Anwar A, Khan NA, Siddiqui R (2019) Brain-eating amoebae infection: challenges and opportunities in chemotherapy. *Mini Rev Med Chem* 19(12):980–987
- Mungroo MR, Shahbaz MS, Anwar A, Saad SM, Khan KM, Khan NA, Siddiqui R (2020) Aryl quinazolinone derivatives as novel therapeutic agents against brain-eating amoebae. *ACS Chem Neurosci* 11(16):2438–2449
- Mungroo MR, Khan NA, Maciver S, Siddiqui R (2022) Opportunistic free-living amoebal pathogens. *Pathogens and Global Health* 116(2):70–84
- BBC NEWS 2020. Brain-eating microbe: US city warned over water supply. [Online] Available at: < <https://www.bbc.co.uk/news/world-us-canada-54313110> > [Accessed 20 November 2023].
- Ong TYY, Khan NA, Siddiqui R (2017) Brain-eating amoebae: predilection sites in the brain and disease outcome. *J Clin Microbiol* 55(7):1989–1997
- Padzik M, Hendiger EB, Chomicz L, Grodzik M, Szmidi M, Grobelny J, Lorenzo-Morales J (2018) Tannic acid-modified silver nanoparticles as a novel therapeutic agent against Acanthamoeba. *Parasitol Res* 117(11):3519–3525
- Patel, D. K., Singh, G. K., Husain, G. M., & Prasad, S. K. (2024). Ethnomedicinal importance of patuletin in medicine: pharmacological activities and analytical aspects. *Endocrine Metabolic & Immune Disorders-Drug Targets (Formerly Current Drug Targets-Immune. Endocrine & Metabolic Disorders)*. 24 519–530.
- Rayamajhee B, Subedi D, Peguda HK, Willcox MD, Henriquez FL, Carnt N (2021) A systematic review of intracellular microorganisms within *Acanthamoeba* to understand potential impact for infection. *Pathogens* 10(2):225
- Razzak, Z.A., Afzal, S.T., Najumuddin, Saifullah, S., Maharjan, R., Bano, S., Faizi, S., Shah, M.R. and Simjee, S.U., 2023. Patuletin from *Tagetes patula*: an inhibitor of MMP-2 and MMP-9 in collagen-induced arthritis rat model and virtual screening analysis. *Revista Brasileira de Farmacognosia*. 1–16.
- Rice CA, Colon BL, Chen E, Hull MV, Kyle DE (2020) Discovery of repurposing drug candidates for the treatment of diseases caused by pathogenic free-living amoebae. *PLoS Negl Trop Dis* 14(9):e0008353
- Sadaf F, Saleem R, Khan RA, Ahmad U, Lubna Bano S, Faizi S (2023) Antihypertensive effect of patulitrin and other constituents from *Tagetes patula* L. (French marigold) in acute L-NAME induced hypertensive rats. *Nat Prod Res* 38(12):2019–2025
- Saifullah S, Kanwal T, Ullah S, Kawish M, Habib SM, Ali I, Munir A, Imran M, Shah MR (2021) Design and development of lipid modified chitosan containing muco-adhesive self-emulsifying drug delivery systems for cefixime oral delivery. *Chem Phys Lipids* 235:105052. <https://doi.org/10.1016/j.chemphyslip.2021.105052>
- Sarink, M.J., van der Meijs, N.L., Denzer, K., Koenderman, L., Tielsen, A.G. and van Hellemond, J.J., 2022. Three encephalitis-causing amoebae and their distinct interactions with the host. *Trends in Parasitology*.
- Siddiqui R, Khan NA (2023) Contact lens disinfectants against Acanthamoeba keratitis: an overview of recent patents and future needs. *Pharm Patent Analyst* 12(3):87–89
- Siddiqui R, Yehia Abouleish M, Khamis M, Ibrahim T, Khan NA (2021) Current medicines hold promise in the treatment of orphan infections due to brain-eating amoebae. *Expert Opin Orphan Drugs* 9:227–235
- Siddiqui R, Boghossian A, Alqassim SS, Kawish M, Gul J, Jabri T, Shah MR, Khan NA (2023) Anti-Balamuthia mandrillaris and anti-Naegleria fowleri effects of drugs conjugated with various nanostructures. *Arch Microbiol* 205(5):170
- Sirelkhatim A, Mahmud S, Seeni A, Kaus NHM, Ann LC, Bakhori SKM, Hasan H, Mohamad D (2015) Review on zinc oxide nanoparticles: antibacterial activity and toxicity mechanism. *Nano-Micro Letters* 7:219–242
- Smith KF, Goldberg M, Rosenthal S, Carlson L, Chen J, Chen C, Ramachandran S (2014) Global rise in human infectious disease outbreaks. *J R Soc Interface* 11(101):20140950
- Souza FR, Fornasier F, Souza LMP, Peñafiel MP, Nascimento JB, Mal-fatti-Gasperini AA, Pimentel AS (2020) Interaction of naringin and naringenin with DPPC monolayer at the air-water interface. *Colloids Surf A Physicochem Eng Asp* 584:124024. <https://doi.org/10.1016/j.colsurfa.2019.124024>
- Taravaud A, Fechtali-Moute Z, Loiseau PM, Pomel S (2021) Drugs used for the treatment of cerebral and disseminated infections caused by free-living amoebae. *Clin Transl Sci* 14(3):791–805
- The Guardian 2020. *Texas Residents Warned Of Tap Water Tainted With Brain-Eating Microbe*. [Online] Available at: <https://www.theguardian.com/us-news/2020/sep/26/texas-tap-water-tainted-brain-eating-microbe?CMP=share_btn_tw> [Accessed 3rd November 2023].
- Visvesvara GS, Schuster FL, Martinez AJ (1993) *Balamuthia mandrillaris*, NG, N. Sp., agent of amebic meningoencephalitis in humans and other animals. *J Eukaryot Microbiol* 40(4):504–514

Publisher's Note Springer Nature remains neutral with regard to jurisdictional claims in published maps and institutional affiliations.

Springer Nature or its licensor (e.g. a society or other partner) holds exclusive rights to this article under a publishing agreement with the author(s) or other rightsholder(s); author self-archiving of the accepted manuscript version of this article is solely governed by the terms of such publishing agreement and applicable law.